



1 Differences in organic carbon fractions and stability explain limited accumulation in loam 2 and sandy loam under greenhouse conditions Boyuan Tan ¹ · Lu Yang ¹ · Xun Xiao ² · Chunji Li ^{3, 4} · Jing Tan ¹ · Ning An ¹ · Lingxuan Meng 3 4 1 · Yanli Yi 1 · Fengkui Qian 5 · Na Li 6 · Xue Liu 7 · Song Li 1* · Wei Han 1* 5 ¹ College of Land and Environment, Shenyang Agricultural University, Shenyang 110866, China 6 ² State Key Laboratory of Soil and Sustainable Agriculture, Institute of Soil Science, Chinese 7 Academy of Sciences, Nanjing 210008, China 8 ³ College of Agriculture and Biology, Zhongkai University of Agriculture and Engineering, 9 Guangzhou, 510550, China ⁴ Key Laboratory of Green Prevention and Control on Fruits and Vegetables in South China, 10 11 Ministry of Agriculture and Rural Affairs, Guangzhou, 510550, China 12 ⁵ School of Humanities and Law, Northeastern University, Shenyang, 110169, China 13 ⁶Liaoning Academy of Agricultural Science, Shenyang, Liaoning 110866, China 14 ⁷Key Liaoning Vocational College of Ecological Engineering, Shenyang 110101, China 15 * Corresponding authors: 16 Song Li; Email: lisong_86@syau.edu.cn 17 Wei Han; Email: hanweiguy@163.com





Abstract

19

20

21

22

23

24

25

26

27

28

29

30

31

32

33

34

35

36

37

38

39

40

Manure is widely applied in greenhouses to enhance soil organic carbon (SOC) and improve fertility. However, how SOC fractions and their chemical stability change under different soil textures and long-term manure inputs remains unclear. We investigated greenhouse soils with 2-50 years of manure application in loam and sandy loam. SOC, easily oxidizable carbon (EOC), microbial biomass carbon (MBC), dissolved organic carbon (DOC), particulate organic carbon (POC), and mineral-associated organic carbon (MAOC) were quantified. The molecular structures of SOC were analyzed via 13C NMR spectroscopy. Results showed that SOC in loam stabilized after about 20 years of manure application, whereas sandy loam reached equilibrium within 2 years. In loam, aromatic C and carbonyl C in SOC increased, raising the aromaticity index (ARM); in sandy loam, alkyl C increased, elevating A/OA and the hydrophobicity index (HI). Loam contained higher SOC, EOC, POC, and MAOC contents than sandy loam, with SOC positively correlated with EOC, POC, and MAOC, whereas in sandy loam SOC was positively correlated only with EOC and MAOC, and negatively with fPOC. In loam, ARM and HI promoted SOC accumulation by stimulating EOC and POC, which enhanced MAOC formation. In sandy loam, HI mainly promoted SOC through increasing EOC, which enhanced MAOC formation. In loam, MAOC formation was mainly associated with POC, whereas in sandy loam it was driven by EOC. Overall, in greenhouses, long-term stability of SOC depends on the transformation of labile carbon into stable fractions, with fine-textured soils exhibiting greater sequestration efficiency due to higher structural stability and greater MAOC accumulation. Keywords: organic carbon sequestration, organic carbon fractions, organic carbon stability, greenhouse soils, long-term manure application

42

43

44

45

46

47

48

49

50

51

52

53

54

55

56

57

58

59

60

61

62





1. Introduction

Soil organic carbon (SOC) is a keystone determinant of soil fertility and sustainable agricultural production; its quantity and composition directly regulate soil fertility and resilience to environmental stress (Beillouin et al., 2023; Oldfield et al., 2019). SOC fractions differ markedly in function. Labile carbon pools (e.g., soil labile organic carbon fractions [SLOCF] and particulate organic carbon [POC]) are highly sensitive to environmental and management perturbations, capturing short-term shifts in soil quality and carbon turnover; whereas stable carbon pools (e.g., mineral-associated organic carbon [MAOC]) reflect the long-term stabilization and preservation of SOC, functioning as the basis for maintaining structural stability and long-term fertility (Das et al., 2023; Zheng et al., 2022; Lavallee et al., 2020; Witzgall et al., 2021). Therefore, compared with SOC content, SOC composition can reveal soil productivity, nutrient supply, and carbon sequestration potential in greater detail. Manure application has been widely demonstrated to significantly enhance SOC content, attributable not only to direct carbon inputs but also to its stimulation of microbial activity and the consequent promotion of organic matter decomposition and resynthesis (Denoncourt et al., 2025; Wu et al., 2024). A global meta-analysis by Gross and Glaser (2021) showed that manure application, on average, enhanced SOC stocks by about 35.4%. Although total SOC increases, the effects of manure application on different carbon fractions are not consistent. Manure application preferentially enriches SLOC and POC, and these labile carbon pools are gradually incorporated into stable pools through microbial reorganization and mineral mediation, serving as important precursors for MAOC formation (Hao et al., 2025; Zhou et al., 2024). At the molecular level, ¹³C Nuclear Magnetic Resonance (NMR) analyses revealed increases in alkyl C, declines in aromatic

64

65

66

67

68

69

70

71

72

73

74

75

76

78

79

80

81

82

83

84





C, higher A/OA, and lower ARM following manure application, suggesting a shift of SOC from aromatic dominance to more hydrophobic and aliphatic structures (Zhao et al., 2023). The efficiency of manure-derived carbon transformation into SOC depends on climatic conditions, soil texture, and agricultural systems. Long-term manure application in non-tropical climates can increase SOC stocks by about 12.8 Mg ha-1, whereas in tropical regions the increase is only about 8.5 Mg ha⁻¹ (Gross and Glaser, 2021). However, Galluzzi et al. (2025) pointed out that although rising temperatures usually accelerate SOC decomposition, SOC accumulation is simultaneously constrained by mineralogical composition. Compared with coarse-textured soils, fine-textured soils (such as loam) possess higher surface area and stronger sorptive capacity, which enable them to more effectively bind low-molecular-weight fractions such as SLOCF and POC into MAOC, thus enhancing SOC long-term storage (Kleber et al., 2015; Islam et al., 2022; Das et al., 2023). Under similar temperature and soil texture conditions, SOC in the 0-20 cm plow layer of paddy soils averages about 9 Mg ha-1 higher than in upland soils., primarily due to the inhibition of SOC mineralization under flooded conditions (Liu et al., 2021). In contrast to open-field agriculture, greenhouses are maintained under consistently warm and humid environments, with air temperatures typically ranging from 18-35°C and relative humidity of approximately 65-80% (Tan et al., 2025; Yang et al., 2024). Such stable and relatively high temperature-humidity regimes enhance microbial activity and substrate decomposition, thereby accelerating SOC turnover. Consequently, to improve soil fertility, manure inputs in greenhouses often reach 30-120 Mg ha-1 yr-1; however, SOC accumulation remains considerably lower than anticipated (Zhang et al., 2022; Tan et al., 2025). Zhang et al. (2022) found that continuous annual application of 37.5 Mg ha⁻¹ of chicken manure resulted in a

86

87

88

89

90

91

92

93

94

95

96

97

98

99

100

101

102

103

104

105

106





new SOC equilibrium after five years, with SOC content increasing by 1.27-fold, yet only 24% of the exogenous carbon was retained. In addition, the majority of greenhouse studies span only 1-10 years, and although apparent equilibrium in total SOC has been observed, such short-term stabilization does not represent an endpoint, as SOC may continue to accumulate or shift over longer timescales. Evidence from open-field studies indicates that net SOC accumulation, particularly MAOC, typically requires continuous organic inputs for more than 20-30 years before becoming pronounced (Dietz et al., 2024; Just et al., 2023). To more comprehensively evaluate the effects of manure application on SOC in greenhouses, it is necessary to analyze SOC accumulation dynamics and carbon fraction distribution over much longer timescales. Accordingly, this study examined greenhouse soils with loam and sandy loam spanning 2-50 years of manure application, employing analyses of SOC fractions (SLOCF, POC, MAOC) combined with ¹³C NMR spectroscopy to systematically compare the composition and molecular structural features of SOC fractions across different manure application years. The aims of this study were: (1) to compare variations in SOC content, structural features, and molecular composition between loam and sandy loam soils in greenhouses under different years of manure application; and (2) to determine the relationships between changes in SOC fractions and molecular structural features with long-term SOC accumulation. The findings will provide a scientific basis for formulating greenhouse manure application strategies and sustaining soil fertility over the long term.

2. Materials and methods

2.1 Site description

The sampling sites for this study were located in Wujianfang Town (41°49'12"N,

108

109

110

111

112

113

114

115

116

117

118

119

120

121

122

123

124

125

126

127

128





120°43'12"E) and Yangshibao Town (41°37'48"N, 122°45'36"E), which are two key regions for greenhouse agriculture in Liaoning Province, northeast China. Greenhouse agriculture has steadily developed in these two regions since 1970 and 1988, respectively, and has gradually expanded with the advancement of farming techniques and improved economic benefits. To improve production efficiency and support local agriculture, the government organized standardized planting schedules, crop rotation, and water-nutrient management training, thus providing ideal conditions for investigating the composition of SOC fractions and their stabilization characteristics under varying durations of manure application in greenhouses. By 2020, the greenhouses in these two regions had planting histories ranging from 2-50 years (Table 1). The soil in Wujianfang Town is classified as Luvisols, while the soil in Yangshibao Town is classified as Cambisols (FAO, 2015). The soil texture was classified based on the proportion of sand, silt, and clay particles in the collected samples, using the United States Department of Agriculture soil texture triangle. Soils in Wujianfang and Yangshibao were classified as loam and sandy loam, respectively (Table 1). Each greenhouse sample plot was 60 m \times 15 m, with an average daytime temperature of 22–36 °C and nighttime temperature of 15–18 °C. A three-crop rotation system of tomato-bean-tomato was implemented annually. Tomato is the main crop, with a planting density of 82,500 plants ha⁻¹. The greenhouses were treated annually with approximately 41.25 Mg ha-1 (dry weight) of mixed cow and pig manure composts, providing a carbon input of 11.58 Mg ha-1 yr-1. The compost contained 28.07% carbon and 2.24% nitrogen. Additionally, chemical fertilizers were applied at annual rates of 300-400 kg ha⁻¹ N, 300-400 kg ha⁻¹ P₂O₅, and 450 kg ha⁻¹ K₂O, in combination with a drip irrigation system. To compare the effects of the greenhouse, open-field





soils located within 100 m of the sampled greenhouse were selected as controls (CK). These control fields followed the same tomato-soybean-tomato rotation, with similar chemical fertilizer application rates but no manure application.

2.2 Soil sampling and analysis

Soil samples were collected in May 2020. Greenhouse plots with similar manure application durations were grouped into loam (Wujianfang Town) and sandy loam (Yangshibao Town) soils. Each group consisted of 6 to 8 samples, for a total of 90 samples. In each greenhouse plot, soil samples were collected from five points arranged in an X-pattern at a depth of 0–20 cm and combined to form a composite sample. To ensure consistency and reduce variability, samples with marked differences in soil texture were excluded, and only soils with a neutral pH (6–8) were retained. This approach was adopted to minimize potential bias from soil property heterogeneity and to ensure the reliability of the experimental results. The same sampling and screening methods for the CK were applied to the CK adjacent to the greenhouse plots. After screening, 42 samples remained. Among these, four samples were collected from greenhouse sandy loam aged 30–32 years, and loam aged 9–11 years and 28–31 years, while the remaining groups consisted of three samples each (Table 1).

2.3 SOC and sequestration analysis

The SOC content was determined using the potassium dichromate ($K_2Cr_2O_7$) oxidation method (Lu, 2000).

SOC stock (SOC_{stock}, Mg C ha⁻¹) was estimated by Eq. (1) (Liu et al., 2015):

$$SOC_{stack} = SOC \times BD \times 0.20 \times 10^4 \times 10^{-3}$$
 (1)





150 Where SOC is the SOC content (g kg⁻¹ soil), BD is the soil bulk density (g cm⁻³), and 0.20 151 is the depth of the plow horizon (m). 10^4 is the conversion factor for hectare to square meters (m²), 152 and 10^{-3} is the overall unit conversion factor for adjusting the units to Mg C ha⁻¹.

SOC sequestration rate (SOCs, %) was estimated using Eq. (2) (Liu et al., 2015; Lu et al.,

154 2009):

153

159

160

161

162

163

164

165

166

168

169

170

171

$$SOC_{S} = \frac{SOC_{stock-n} - SOC_{stock-CK}}{C - input_{n}} \times 100$$
 (2)

Where $SOC_{stock-n}$ and $SOC_{stock-CK}$ represent the carbon stocks (Mg C ha⁻¹) in greenhouse soil

with n years of manure application and in the control group, respectively. *C-input_n* represents the

cumulative C input from manure application over n years (Mg C ha⁻¹).

2.4 Fraction of SOC

The SLOCF (EOC, DOC, and MBC), POC (cPOC and fPOC), and MAOC was separated from the soil samples and measured to evaluate the long-term impact of manure application on the turnover and accumulation of different forms of SOC in the greenhouse.

KMnO₄ oxidation method (Vieira et al., 2007) was used to measure EOC in the samples. The fumigation extraction method (Vance et al., 1987) was used to measure DOC and MBC in the samples. DOC content was determined using the extract from the non-fumigated samples. MBC content was estimated using Eq. (3):

$$MBC = \frac{OC_{\rm f} - DOC}{0.45} \tag{3}$$

where OC_f and DOC represent the organic carbon (OC) contents of the fumigated and non-fumigated samples, respectively (g kg⁻¹ soil), and 0.45 is a constant value representing the OC extraction efficiency.

The contents of POC and MAOC were measured using a particle size fractionation method.

173

174

175

176

177

178

179

180

181

182

183

184

185

186

187

188

189

190

191

192

193





An air-dried soil sample (10 g) was placed in a 50 mL centrifuge tube, and 35 mL of 1.85 g cm⁻³ NaI solution (85 g NaI dissolved in 100 mL of water) was added. After shaking the tube 10 times, the sample was centrifuged at 4000 rpm for 20 minutes. The NaI solution was then removed, and the residue on the tube wall was rinsed. The remaining soil was rinsed 2-3 times with deionized water and then treated with 30 mL of 5 g $L^{\text{-1}}$ Na₆P₆O₁₈ solution, followed by shaking at 200 rpm for 18 hours to disperse aggregates. The dispersion was successively sieved through 250 μm and 53 μm mesh sieves. Different fractions were collected: cPOC >250 μm, fPOC 250-53 μm, and MAOC <53 µm. Each fraction was dried at 40 °C to constant weight. The carbon content of each fraction was determined using the K₂Cr₂O₇ oxidation method. The contributions of each carbon fractions (SLOCF, POC, and MAOC) to SOC (%) was estimated using Eq. (4): Proportion SLOCF, POC, MAOC (%) SOC Fraction (SLOCF, POC , MAOC) ×100 (4) 2.5 13C NMR analysis and spectral indicators The molecular structure of SOC was characterized using Cross-Polarization-Magic Angle Spinning (CPMAS) solid-state ¹³C NMR spectroscopy (Bruker AVANCE III 400, Switzerland). To remove paramagnetic materials and concentrate OC, soil samples were pretreated with 10% hydrofluoric acid (HF) solution (Schmidt et al., 2011). The processed samples were dried to constant weight at 40 °C, sieved through a 60-mesh sieve, and stored for NMR analysis. The processed samples were analyzed on a Bruker AVANCE III 400 NMR spectrometer (Switzerland), operating at a ¹³C resonance frequency of 100 MHz, equipped with a 4 mm CPMAS probe. The measurement parameters included a 5 kHz MAS rotation rate, 1 ms contact





time, 0.8 s recovery delay, and 140,000 scans. The spectra were divided into 4 chemical shift regions, with each chemical shift region and its corresponding label as follows: alkyl C (0–45 ppm), O-alkyl C (45–110 ppm), aromatic C (110–160 ppm) and carbonyl C (160–220 ppm). The relative intensities of each SOC structure were calculated by integrating the areas of these regions. Three SOC stability indicators were calculated: the aromaticity index (ARM), hydrophobicity index (HI) (Mustafa et al., 2022), and the ratio of alkyl C to O-alkyl C (A/OA) (Kubar et al., 2018).

2.6 Statistical analysis

Statistical analyses were performed using IBM SPSS Statistics 22 software (IBM, Armonk, New York, USA). Significant differences among treatments were analyzed using one-way analysis of variance (ANOVA) with Tukey's HSD post hoc test for multiple comparisons. Data visualization and Pearson correlation analysis were performed using OriginPro 2023 (OriginLab Corp., Northampton, MA, USA). Pearson correlation coefficients (r) and their significance levels (P) were calculated and visualized as a heatmap. The circle size indicates the strength of the correlation, and the color gradient (red for positive and blue for negative correlations) represents the direction. Statistically significant correlations are marked with asterisks (* for P < 0.05, ** for P < 0.01, *** for P < 0.001). Solid-state 13 C NMR spectra were processed and integrated using MestreNova software (Mestrelab Research, Santiago de Compostela, Spain).

The partial least squares structural equation model (PLS-SEM) was used to explore the pathways by which SOC fractions (SLOCF, POC, and MAOC) and structural stability indices of organic carbon (ARM, HI, and A/OA) influence SOC content in greenhouse. Based on our

hypotheses, an a priori model was first constructed (Fig. S1). The model was subsequently





modified and simplified according to external model quality (heterotrait-monotrait ratio, composite reliability, Cronbach's alpha, and convergent validity), internal model quality (explained variance, R²), and model fit (standardized root mean square residual, SRMR, and normed fit index, NFI). The model was constructed using the R package "plspm" (Hair et al., 2022).

3. Results

3.1 SOC content and sequestration in the greenhouse

In the greenhouse, SOC content did not continuously increase with the prolonged application of manure, and the SOC stock remained much lower than the carbon input from manure application. In the loam, after 20 years of manure application, SOC content stabilized between 33.1–37.0 g kg⁻¹, with a SOC stock of approximately 77.5 Mg C ha⁻¹, and SOCs at 16.1% (Fig. 1a, b). Although both SOC content and stock stabilized after 20 years, SOCs continued to decrease annually with the prolonged application of manure. After 48–50 years of manure application, SOCs decreased to 7.2% (Fig. 1c). In contrast, the effect of manure application on SOC content was relatively weak in the sandy loam. After 2 years of manure application, the SOC content and stock in the sandy loam were 13.3 g kg⁻¹ and 33.0 Mg C ha⁻¹, respectively, representing only 42.2% and 42.6% of those in the loam (Fig. 1a, b). Although SOCs was higher in the sandy loam (54.9%) after 2 years of manure application, it markedly decreased as the application years increased. After approximately 30 years, SOCs in the sandy loam decreased to 4.0%, only 49.2% of that in the loam (Fig. 1c).

3.2 Dynamic changes in SLOCF, POC, and MAOC in the greenhouse

The application of manure enhanced SOC content of various fractions in the greenhouse.

239

240

241

242

243

244

245

246

247

248

249

250

251

252

253

254

255

256

257

258

259





SLOCF took the shortest time to reach a new equilibrium, followed by POC, with MAOC requiring the longest. Specifically, DOC and MBC contents in both soil textures stabilized after 2 years of manure application in greenhouses. EOC stabilized after 9-11 years in loam (5.77-6.92 g kg-1), whereas sandy loam required 21-24 years to reach equilibrium (3.67-4.60 g kg-1), representing only 32% of the loam's (Fig. 2c). In loam, cPOC and fPOC contents reached their peak (5.01 and 6.80 g kg⁻¹) after 28-31 and 20-23 years of manure application, respectively, and then slightly decreased (Fig. 2d, f). In sandy loam, cPOC content remained at 1.19-1.62 g kg⁻¹ within 2-32 years; the fPOC content reached its peak (3.08 g kg⁻¹) at 2 years and significantly decreased to 1.81 g kg⁻¹ at 30-32 years (Fig. 2d, f). In loam, MAOC content gradually stabilized after 28 years of manure application, and reached highest (21.83 g kg⁻¹) after 48-50 years (Fig. 2h). In sandy loam, MAOC content tended to stabilize after 4 years of manure application, maintaining at 6.21-7.54 g kg⁻¹ (Fig. 2h). Compared to sandy loam, loam exhibited significantly higher contents of all OC fractions except DOC and MBC. Sandy loam showed 62.38%, 60.55%, and 65.41% reductions in cPOC, fPOC, and MAOC contents, respectively, relative to loam (Fig. 2a, b). In the greenhouse, the proportion of OC fractions in SOC follows the order: MAOC > EOC > fPOC > cPOC > DOC > MBC. In SLOCF, the proportion of DOC and MBC in SOC peaked at 2 years of manure application in both soil textures and then declined to levels similar to those of CK. The proportion of EOC in SOC significantly increased in the greenhouse, with the increase in the sandy loam being significantly higher than that in the loam (Fig. 3a, b). In the loam, the proportion of cPOC and fPOC in SOC reached 14.1% and 20.0%, respectively, after 20-23 years of manure application, and then decreased to 12.2% and 16.3% after 48-50 years. In





contrast, the proportion of MAOC in SOC gradually increased. Notably, when manure application was less than 48 years, the proportion of MAOC remained lower than that in CK (Fig. 3c). In the sandy loam, the proportion of cPOC and fPOC peaked at 12.7% and 24.5%, respectively, after 2 years of manure application, and then declined. Over 4–32 years, the proportions of cPOC and fPOC remained consistently at 9%–10% and 14%–15%, respectively. MAOC reached its maximum value of 52.3% after 4–6 years of manure application and then stabilized between 47% and 51% thereafter (Fig. 3e).

3.3 Correlations among SOC, SLOCF, POC, and MAOC in the greenhouse

In greenhouses with loam, SOC was highly positively correlated with EOC, cPOC, fPOC, and MAOC (P < 0.001). Among them, MAOC showed the strongest correlation with SOC. Additionally, SOC was significantly positively correlated with cPOC/SOC and fPOC/SOC, and negatively correlated with DOC/SOC and MBC/SOC (P < 0.01, Fig. 4a). In contrast, SOC was only highly positively correlated with MAOC in the sandy loam (P < 0.001). No significant correlation was found between cPOC and either SOC or MAOC, while fPOC was negatively correlated with both SOC and MAOC (P < 0.05). The MAOC/SOC was significantly positively correlated with SOC (P < 0.05), while cPOC/SOC and fPOC/SOC were significantly negatively correlated with SOC (P < 0.01, Fig. 4b).

3.4 Chemical composition and stability of SOC based on ¹³C NMR analysis

The solid-state ¹³C NMR spectra and the relative contributions of various carbon functional groups in SOC are shown in Fig. 5a and 5b, and Table 2. The 0–45 ppm region corresponds to the alkyl C group, predominantly consisting of CH₂ bonds, which are characteristic of branched aliphatic C functional groups. The 45–110 ppm region corresponds to the O-alkyl C group,

283

284

285

286

287

288

289

290

291

292

293

294

295

296

297

298

299

300

301

302

303





such as guaiacol and vanillin, as well as C-N bonds in amino acids. The aromatic C group is prominent in the 110-160 ppm range and is strongly associated with aromatic C and phenolic C structures. The 160-220 ppm region is predominantly dominated by the carbonyl C group, including amides, carboxylic acids, and esters. Long-term manure application significantly altered the distribution of OC functional groups in greenhouse soils, with notable variations observed between different soil textures (Fig. 5a, b). Compared to CK, the proportion of alkyl C in the loam decreased by 13.9% at 9-11 years of manure application, and subsequently increased by 2.6% at 28-31 years. The proportion of O-Alkyl C exhibited a gradual decline, decreasing by 16.7% at 28-31 years. In contrast, the proportions of aromatic C and carbonyl C steadily increased, rising by 17.5% and 10.5%, respectively, at 28-31 years (Table 2). In the sandy loam, manure application increased the proportion of alkyl C while decreasing the proportions of O-alkyl C and aromatic C. Compared to CK, the proportion of alkyl C increased by 12.9% at 30-32 years, while the proportions of O-alkyl C and aromatic C decreased by 6.2% and 5.3%, respectively. The proportion of carbonyl C remained relatively stable, maintaining at 15.56%-19.11% (Table 2). In the loam, long-term manure application primarily increased ARM, followed by HI and A/OA. ARM increased with the extension of manure application years. HI increased only between 28-31 years, remaining relatively stable at 2 years and 9-11 years. A/OA decreased at 2 and 9-11 years. Compared to CK, after 28-31 years of manure application in the greenhouse, ARM, HI, and A/OA increased by 249.44%, 29.39%, and 49.90%, respectively, with an overall increase of 54.61% in SOC stability (Fig. 5c). In contrast, the SOC stability indicators in the sandy loam were

typically associated with methoxy C/N-alkyl compounds, mainly derived from lignin derivatives

305

306

307

308

309

310

311

312

313

314

315

316

317

318

319

320

321

322

323

324

325





significantly lower than those in the loam. In the sandy loam, ARM decreased with the extended manure application years, while HI and A/OA gradually increased. Compared to CK, although the ARM of greenhouse soils after 30-32 years of manure application decreased by 0.12, HI and A/OA increased by 0.29 and 0.99, respectively (Fig. 5d). There were significant differences in the correlation patterns between the two soil textures. In the loam, SOC and all its fractions were significantly negatively correlated with alkyl C and O-alkyl C, but showed highly significant positive correlations with aromatic C and carbonyl C (P < 0.001, Fig. 6a). All SOC fractions were significantly positively correlated with ARM, but negatively with A/OA. HI was significantly positively correlated only with SOC, POC, and MAOC, but not with SLOCF (EOC, DOC, and MBC, Fig. 6a). In contrast, in the sandy loam, POC showed generally weak correlations with functional groups and stability indices; only cPOC was significantly positively correlated with alkyl C and HI, and negatively with O-alkyl C (Fig. 6b). SOC, SLOCF, and MAOC were positively correlated with alkyl C, but generally negatively with O-alkyl C, aromatic C, and carbonyl C. Notably, DOC showed no significant correlation with either aromatic C or carbonyl C. The strongest correlation was observed between carbonyl C and MAOC (P < 0.001), but correlations with other SOC fractions were weak. SOC, SLOCF, and MAOC were all significantly positively correlated with HI, but negatively with ARM. A/OA exhibited significant positive correlations with SOC, EOC, MBC, and MAOC, but was not significantly associated with DOC (Fig. 6b). 3.5 Pathways of long-term SOC storage in greenhouses In loam, SOC content was primarily driven by MAOC and EOC. Although no direct path was found from POC to SOC, SOC stability indices (ARM and HI) exerted significant positive

327

328

329

330

331

332

333

334

335

336

337

338

339

340

341

342

343

344

345

346

347





effects on POC accumulation, and POC indirectly contributed to SOC content through its promotion of MAOC formation. By contrast, the path from MAOC to EOC was not significant (Fig. 7a). In sandy loam, SOC content was jointly influenced by MAOC and POC. SOC stability (HI) significantly enhanced EOC accumulation, which subsequently promoted MAOC formation and ultimately increased SOC content. However, the path between SOC stability (HI) and cPOC showed relatively low significance, and no direct association was detected between cPOC and MAOC (Fig. 7b). 4. Discussion 4.1 Effects of manure application on SOC composition and chemical structure in greenhouse soils Manure application in greenhouses significantly increased SOC content, playing a key role in enhancing soil fertility. However, with continuous application, SOC in loam stabilized after 20 years, whereas in sandy loam equilibrium was reached within only 2 years (Fig. 1). This stabilization likely reflects a new balance in SOC, where additional carbon inputs are offset by the higher mineralization rates characteristic of greenhouse soils (Stewart et al., 2007). The difference in equilibrium time can be attributed to soil texture: fine-textured soils (e.g., loam) provide more binding sites that enhance SOC stability and slow decomposition, while sandy loam, with limited binding capacity, undergoes faster SOC decomposition and therefore reaches equilibrium more rapidly (Wiesmeier et al., 2019; Mao et al., 2024). Manure application significantly increased the contents of SOC fractions in greenhouse soils. Among them, MAOC represented the highest content and proportion (Fig. 2, 3), indicating that

MAOC plays a central role in long-term carbon sequestration in greenhouse soils. This finding is

349

350

351

352

353

354

355

356

357

358

359

360

361

362

363

364

365

366

367

368

369





consistent with previous studies highlighting the dominant role of MAOC in SOC stabilization. Manure application promotes the complexation of OC with mineral oxides, thereby significantly enhancing the stability of MAOC and effectively facilitating SOC sequestration (Zhang et al., 2011). With prolonged manure application, EOC, cPOC, and fPOC and their relative proportions in SOC tended to stabilize (Fig. 2, 3). This phenomenon can be attributed to the rapid turnover characteristics of EOC and POC combined with greenhouse conditions. Manure-derived EOC and POC are more prone to microbial decomposition under elevated temperatures, and with prolonged manure application, their inputs and losses eventually reach a dynamic balance, thereby suppressing further increases in their contents and relative contributions to SOC (Zheng et al., 2022; Zhou et al., 2024). In contrast to the other carbon fractions, DOC and MBC contents showed no significant differences across manure application durations or soil textures (Fig. 2e, g), accounting for less than 2.5% of SOC, indicating that they are mainly regulated by the amount of manure applied. Although their contributions are limited, they could serve as indicators of microbial metabolism and carbon transformation processes (Francioli et al., 2016; Li et al., 2021; Yan et al., 2023). For example, Wu et al. (2024) reported that organic matter addition altered the relative abundances of Bacteroidetes and Acidobacteria, thereby affecting the expression of key carbon-cycle genes such as cbbL and cbbM, which in turn regulated the distribution of carbon fractions. Although the trends of SOC fraction dynamics were generally consistent between the two soil textures, their distribution patterns differed significantly. Loam exhibited significantly higher levels of EOC, POC, and MAOC, and the sustained increase in the proportion of MAOC with prolonged manure application reflects an enhanced capacity for soil organic matter accumulation https://doi.org/10.5194/egusphere-2025-5094 Preprint. Discussion started: 3 November 2025 © Author(s) 2025. CC BY 4.0 License.

370

371

372

373

374

375

376

377

378

379

380

381

382

383

384

385

386

387

388

389

390

391





and stabilization within persistent carbon pools. In contrast, sandy loam contained lower levels of these fractions, indicating a markedly limited potential for long-term SOC sequestration. This is consistent with the findings of Zhou et al. (2024), who reported that light-textured soils are less effective in sequestering SOC due to insufficient clay content and adsorption sites. A global cropland study by Ling et al. (2025) further demonstrated that fine-textured soils with higher proportions of clay and silt provide more binding and protective sites for organic matter, thereby promoting the formation and stabilization of MAOC. In contrast, sandy soils with limited binding sites tend to store SOC predominantly in free particulate forms, which further explains the observed differences in SOC fractions between loam and sandy loam in this study. Manure application not only altered SOC and its fractions but also significantly modified the composition of SOC functional groups. In the loam, the application of manure decreased the proportion of alkyl C and O-alkyl C in SOC, while increasing the proportions of aromatic C and carbonyl C (Fig. 5a, Table 2). O-alkyl C mainly originates from cellulose, peptides, and other unstable organic components. Alkyl C derives from primary plant bio-polymers and metabolic products of soil microorganisms. In comparison with the more resistant aromatic C and carbonyl C, they can be preferentially biodegraded (Panettieri et al., 2014; Lan et al., 2022). Alkyl C and O-alkyl C gradually transform into more stable forms of OC through oxidation by enzymes secreted by microorganisms and reactive oxygen species. For instance, Yao et al. (2022) found that in the process of OC decomposition by microorganisms, oxidation reactions and free radical reactions in the soil can also convert compounds containing alkyl C into carbonyl-containing compounds (such as ketones and aldehydes), thereby promoting the formation of aromatic C structures. At the early stage of manure application (approximately 2 years), the ARM of SOC in loam increased,

393

394

395

396

397

398

399

400

401

402

403

404

405

406

407

408

409

410

411

412

413





to the rapid decomposition of large amounts of labile components (e.g., O-alkyl C and alkyl C) under the high-temperature conditions of greenhouses, leading to a relative increase in the proportion of aromatic C (Xu et al., 2020). With the extension of manure application years, the alkyl C and carbonyl C structures in SOC gradually rose, ultimately improving the stability of SOC. The changes in the proportions of SOC functional groups in the sandy loam exhibited characteristics distinct from those in the loam. The proportion of alkyl C gradually increased with prolonged manure application, whereas the proportions of O-alkyl C, aromatic C, and carbonyl C show an overall decreasing trend (Fig. 5b, Table 2). This is likely because of the lower content of clay and silt in the sandy loam, which reduces the physical protection of soil particles on SOC (An et al., 2021; Yao et al., 2022). In sandy loam, manure application significantly altered HI, A/OA, and ARM, with HI and A/OA increasing but ARM decreasing, in contrast to loam (Fig. 5d). This indicates that, although manure application in the sandy loam does not favor the formation of the most stable aromatic C, it has a positive effect on SOC stability by enhancing its hydrophobicity and increasing the proportion of alkyl C. Previous studies have also demonstrated that alkyl C, as a major contributor to thermal stability and hydrophobicity, can enhance the resistance of SOC to decomposition in soil (Almendros and González-Pérez, 2025). These results suggest that loam, due to its higher clay and silt contents, not only facilitates the gradual transformation of EOC and POC into MAOC but also achieves long-term SOC stabilization through the accumulation of recalcitrant structures such as aromatic C and carbonyl C. In contrast, sandy loam, constrained by limited binding sites, exhibits lower levels of SOC fractions and

while the HI and A/OA were significantly lower than those in the CK (Fig. 5c). This may be due





414 structural stability, relying more on hydrophobic stabilization driven by alkyl C, which results in 415 markedly lower SOC sequestration potential compared with loam. 416 4.2 Correlations between SOC fractions and chemical structures and sequestration 417 pathways in greenhouse soils 418 In the loam, the higher clay and silt contents significantly enhanced the capacity for SOC 419 accumulation, mainly attributable to mineral protection driven by soil texture (Datta et al., 2017; 420 Yan et al., 2023). Although SLOCF and POC are generally difficult to preserve in soils over the 421 long term, these fractions continuously associate with mineral particles during decomposition and 422 form more stable MAOC through processes of adsorption, aggregation, and re-precipitation (Zhou 423 et al., 2024; Six et al., 2002). Consequently, MAOC showed significant positive correlations with 424 EOC, cPOC, and fPOC (Fig. 4a). Previous studies have shown that cPOC and fPOC initially 425 attach to the surfaces of clay and silt particles, gradually forming stable MAOC through 426 physicochemical interactions such as cation bridging, hydrogen bonding, and van der Waals 427 forces (Six et al., 2002; Rocci et al., 2021; Zhou et al., 2024). Additionally, SLOCF, particularly 428 POC derived from DOC, can also enter the POC pool and further enhance SOC stability by 429 facilitating MAOC formation (Si et al., 2024). These precursor-product linkages directly 430 influence the long-term stability of SOC in loam (Ji et al., 2024; Si et al., 2024). 431 In contrast, the sandy loam, with its low clay and silt contents, exhibited a weaker SOC 432 accumulation capacity, where SOC was positively correlated only with EOC and MAOC, but 433 negatively correlated with fPOC (Fig. 4b). This finding differs from the results of Rocci et al. 434 (2021), who reported that increases in both MAOC and POC directly contributed to SOC pool 435 enhancement. However, in the sandy loam soil under greenhouses in this study, the negative

437

438

439

440

441

442

443

444

445

446

447

448

449

450

451

452

453

454

455

456

457





correlation between POC and MAOC suggests that the accumulation of POC may not have contributed to effective stabilization, but rather may have accelerated the decomposition of existing MAOC. This interpretation is supported by Angst et al. (2023), who indicated that continuous addition of exogenous organic matter to soils approaching carbon saturation could trigger a microbial priming effect, thereby accelerating MAOC mineralization. Furthermore, ¹³C tracer experiments have shown that low-quality litter (e.g., plant residues with high lignin content and high C/N ratios) can induce strong priming effects, accelerating MAOC loss and offsetting the newly formed MAOC (Elias et al., 2024). In addition, Liang et al. (2023) found that in soils dominated by low-reactivity clays, rhizodeposition-derived bioavailable carbon inputs can deplete the MAOC pool, indicating that limited mineral protection capacity increases the susceptibility of MAOC to carbon-induced mobilization. This study also found that the correlations between SOC fractions, functional groups, and stability indices differed significantly between loam and sandy loam (Fig. 6). Previous studies have shown that fine-textured soils, particularly within the MAOC fraction, tend to accumulate microbial transformation products and chemically restructured stable compounds such as carboxyl, aromatic, and long-chain alkyl groups, whereas coarse-textured soils preferentially retain partially decomposed plant residues, leading to higher proportions of O-alkyl C (Jindaluang et al., 2013; Niu et al., 2024; Witzgall et al., 2021). In this study, EOC, POC, and MAOC in loam showed significant positive correlations with SOC stability indices such as ARM and HI (Fig. 6a), indicating that even metabolically active fractions may contribute to long-term SOC stabilization through mineral associations when mineral adsorption sites are abundant. In contrast, the organic carbon fractions in sandy loam were mainly positively correlated with alkyl C, HI, and A/OA,

459

460

461

462

463

464

465

466

467

468

469

470

471

472

473

474

475

476

477

478

479





while fPOC showed no significant relationships with SOC chemical structures or stability indices (Fig. 6b), indicating that these particulate organic carbons were not effectively adsorbed or protected. This finding aligns with Witzgall et al. (2021), who observed in controlled litter decomposition experiments that fine-textured soils preferentially retained microbially restructured SOC, whereas coarse-textured soils released more CO2 and retained only limited plant-derived fragments. In loam and sandy loam, MAOC represents the primary driver of SOC accumulation, but the contribution pathways of EOC and POC differ markedly (Fig. 7). In loam, although EOC can be partially transformed into residues and incorporated into MAOC through microbial metabolism, its contribution is not significant. This does not imply the absence of such a process; rather, the abundant clay and mineral binding sites in loam make the microbial reprocessing and mineral association of POC the predominant sources of MAOC, thereby masking the effect of EOC incorporation (Liu et al., 2025; Zhou et al., 2024). Therefore, the role of EOC in loam is mainly reflected in its short-term enhancement of SOC content, while the long-term accumulation of MAOC relies more on the transformation of POC and mineral protection. In contrast, in sandy loam, the limited clay and sorption sites markedly reduce the efficiency of POC conversion into MAOC, resulting in POC remaining largely in the form of particulate residues (Christy et al., 2023; Fohrafellner et al., 2024). This explains why there was no significant path detected between POC and MAOC in sandy loam, while POC still directly promoted SOC content through its own accumulation. Under such conditions, the molecular characteristics of EOC, such as small molecules rich in carboxyl and phenolic hydroxyl groups, enable rapid diffusion and preferential occupation of scarce mineral binding sites, making it a key precursor of MAOC (Christy et al.,

481

482

483

484

485

486

487

488

489

490

491

492

493

494

495

496

497

498

499

500

501





2023). This is consistent with several studies reporting that in soils with low fine particle content, inputs of labile or soluble organic carbon contribute relatively more to the stable carbon pool (Peng et al., 2025; Simon et al., 2025). In summary, the results of this study indicate that the long-term stabilization of SOC in greenhouse soils is not the accumulation of a single carbon pool, but rather a synergistic process in which labile carbon fractions serve as substrates that are gradually incorporated into stable pools through microbial metabolism and transformation, thereby achieving long-term preservation. The results of this study provide guidance for the management of manure application in greenhouse soils with different textures. It should be noted that this study did not include structural characterization of submicron-scale mineral-OC complexes (e.g., X-ray absorption fine structure spectroscopy), and therefore could not distinguish the differences among clay mineral types (e.g., montmorillonite vs. kaolinite) in the formation and stabilization of MAOC. In addition, this study primarily analyzed the relationship between SOC fractions and stabilization, lacking direct evidence on the microbial communities driving carbon transformation. Future studies could integrate metagenomic sequencing techniques to elucidate the community structure and metabolic traits of functional microorganisms that play key roles in carbon transformation across soils with different textures, thereby advancing the understanding of SOC stabilization processes in greenhouses through a multi-scale approach. 5. Conclusions In greenhouse soils, SOC content gradually stabilized with increasing years of manure application, with loam reaching equilibrium after approximately 20 years, whereas sandy loam

attained a new balance within only 2 years. Under equivalent manure inputs, loam contained

503

504

505

506

507

508

509

510

511

512

513

514

515

516

517

518

519

520

521

522

523





significantly higher amounts of EOC, POC, and MAOC than sandy loam, with SOC stocks being approximately 2-3 times higher. In loam, SOC showed significant positive correlations with EOC, POC, and MAOC, indicating their synergistic role in long-term SOC stabilization. By contrast, in sandy loam, SOC was positively associated only with EOC and MAOC, but negatively with fPOC, reflecting the limited capacity of sandy loam to incorporate POC into the stable pool under constrained clay and sorption sites. Further analysis revealed that manure application in loam enriched aromatic and carbonyl C, a structural feature conferring greater stability and enhancing the efficiency of EOC and POC transformation into MAOC, thereby facilitating long-term SOC accumulation. Conversely, SOC in sandy loam was dominated by hydrophobic alkyl C, where increases in HI primarily stimulated EOC accumulation, and SOC stabilization largely depended on the continuous replenishment of EOC and its derivatives. Taken together, these findings demonstrate that long-term SOC sequestration is not determined solely by the quantity of external inputs, but is strongly governed by the efficiency with which labile fractions are transformed into MAOC. Overall, the response of greenhouse SOC to long-term manure application is essentially regulated by both the distribution of C fractions and the structural stability of their chemical composition. Data availability Data will be made available on request. **Author contribution:** Conceptualization: Yanli Yi, Song Li, Wei Han; Data curation: Boyuan Tan; Formal analysis: Boyuan Tan, Lu Yang, Xun Xiao, Lingxuan Meng; Funding acquisition: Song Li, Wei Han;

Investigation: Boyuan Tan, Lu Yang, Lingxuan Meng, Jing Tan; Methodology: Boyuan Tan;





524	Project administration: Song Li, Wei Han; Resources: Song Li, Wei Han; Software: Boyuan Tan;
525	Supervision: Yanli Yi, Wei Han; Validation: Boyuan Tan; Visualization: Boyuan Tan, Lu Yang;
526	Writing – original draft: Boyuan Tan; Writing – review & editing: Xue Liu, Fengkui Qiani, Na Li,
527	Chunji Li, Ning An, Song Li, Wei Han.
528	Competing interests
529	The authors declare that they have no known competing financial interests or personal
530	relationships that could have appeared to influence the work reported in this paper.
531	Acknowledgement
532	The authors gratefully acknowledge the College of Land and Environment, Shenyang Agricultural
533	University, for providing research facilities and academic support. We also thank the colleagues
534	and technical staff for their assistance with field sampling, laboratory analyses, and data
535	processing.
536	Financial support
537	This research was financially supported by the National Natural Science Foundation of China
538	(Grant No. U23A2053), the National Key Research and Development Program of China (Grant
539	No.2023YFD1500303), and the Scientific Research Project of Science and Technology of
540	Liaoning Province (Grant No. 2022-MS-254).
541	References
542	Almendros, G., González-Pérez, J. A.: Soil organic carbon sequestration mechanisms and the
543	chemical nature of soil organic matter—A review, Sustainability, 17, 6689,
544	https://doi.org/10.3390/su17156689, 2025.





545	An, Z., Bernard, G. M., Ma, Z., Plante, A. F., Michaelis, V. K., Bork, E. W., Carlyle, C. N.,
546	Baah-Acheamfour, M., Chang, S. X.: Forest land-use increases soil organic carbon
547	quality but not its structural or thermal stability in a hedgerow system, Agric. Ecosyst.
548	Environ., 321, 107617, https://doi.org/10.1016/j.agee.2021.107617 , 2021.
549	Angst, G., Mueller, K. E., Castellano, M. J., Vogel, C., Wiesmeier, M., Mueller, C. W.:
550	Unlocking complex soil systems as carbon sinks: multi-pool management as the key, Nat.
551	Commun., 14, 2967, https://doi.org/10.1038/s41467-023-38700-5, 2023.
552	Beillouin, D., Corbeels, M., Demenois, J., Berre, D., Boyer, A., Fallot, A., Feder, F., Cardinael, R.:
553	A global meta-analysis of soil organic carbon in the Anthropocene, Nat. Commun., 14,
554	3700, https://doi.org/10.1038/s41467-023-39338-z, 2023.
555	Christy, I., Moore, A., Myrold, D., Kleber, M.: A mechanistic inquiry into the applicability of
556	permanganate oxidizable carbon as a soil health indicator, Soil Sci. Soc. Am. J., 87,
557	1083–1095, https://doi.org/10.1002/saj2.20569, 2023.
558	Das, A., Purakayastha, T. J., Ahmed, N., Das, R., Biswas, S., Shivay, Y. S., Sehgal, V. K., Rani,
559	K., Trivedi, A., Tigga, P., et al.: Influence of clay mineralogy on soil organic carbon
560	stabilization under tropical climate, Indian J. Soil Sci. Plant Nutr., 23, 1003-1018,
561	https://doi.org/10.1007/s42729-022-01099-x, 2023.
562	Datta, R., Kelkar, A., Baraniya, D., Molaei, A., Moulick, A., Meena, R. S., Formanek, P.:
563	Enzymatic degradation of lignin in soil: A Review, Sustainability, 9, 1163,
564	https://doi.org/10.3390/su9071163, 2017.
565	Denoncourt, C., Chantigny, M. H., Angers, D. A., Maillard, É., Halde, C.: Animal manure
566	application promotes nitrogen and organic carbon accumulation in soil organic matter





567	fractions: A global meta-analysis, Sci. Total Environ., 996, 180097,
568	https://doi.org/10.1016/j.scitotenv.2025.180097, 2025.
569	Dietz, C. L., Jackson, R. D., Ruark, M. D., Sanford, G. R.: Soil carbon maintained by perennial
570	grasslands over 30 years but lost in field crop systems in a temperate Mollisol, Commun.
571	Earth Environ., 5, 360, https://doi.org/10.1016/j.scitotenv.2025.180097 , 2024.
572	Elias, D. M. O., Mason, K. E., Goodall, T., Taylor, A., Zhao, P., Otero-Fariña, A., Chen, H.,
573	Peacock, C. L., Ostle, N. J., Griffiths, R., et al.: Microbial and mineral interactions
574	decouple litter quality from soil organic matter formation, Nat. Commun., 15, 10063,
575	https://doi.org/10.1038/s41467-024-54446-0, 2024.
576	Fohrafellner, J., Keiblinger, K. M., Zechmeister-Boltenstern, S., Murugan, R., Spiegel, H.,
577	Valkama, E.: Cover crops affect pool specific soil organic carbon in cropland - A
578	meta-analysis, Eur. J. Soil Sci., 75, e13472, https://doi.org/10.1111/ejss.13472, 2024.
579	FAO (Food and Agriculture Organization of the United Nations): World reference base for soil
580	resources 2014: International soil classification system for naming soils and creating
581	legends for soil maps, World Soil Resources Reports No. 106, FAO, Rome, 2014.
582	Francioli, D., Schulz, E., Lentendu, G., Wubet, T., Buscot, F., Reitz, T.: Mineral vs. organic
583	amendments: Microbial community structure, activity and abundance of agriculturally
584	relevant microbes are driven by long-term fertilization strategies, Front. Microbiol., 7,
585	1446, https://doi.org/10.3389/fmicb.2016.01446, 2016.
586	Galluzzi, G., Plaza, C., Giannetta, B., Priori, S., Zaccone, C.: Time and climate roles in driving
587	soil carbon distribution and stability in particulate and mineral-associated organic matter





588	pools, Sci. Total Environ., 963, 178511, https://doi.org/10.1016/j.scitotenv.2025.178511,
589	2025.
590	Gross, A., Glaser, B.: Meta-analysis on how manure application changes soil organic carbon
591	storage, Sci. Rep., 11, 5516, https://doi.org/10.1038/s41598-021-82739-7, 2021.
592	Hair, J. F., Hult, G. T. M., Ringle, C. M., Sarstedt, M.: A primer on partial least squares structural
593	equation modeling (PLS-SEM), 3rd ed., Sage Publications, Thousand Oaks, CA, USA,
594	2022.
595	Hao, X., Ma, X., Sun, L., Liu, S., Ji, J., Zhou, B., Zhao, Y., Zheng, Y., Kuang, E., Liu, Y., et al.:
596	High ratio of manure substitution enhanced soil organic carbon storage via increasing
597	particulate organic carbon and nutrient availability, Plants, 14, 2045,
598	https://doi.org/10.3390/plants14132045, 2025.
599	Islam, M. R., Singh, B., Dijkstra, F. A.: Stabilisation of soil organic matter: interactions between
600	clay and microbes, Biogeochemistry, 160, 145–158,
601	https://doi.org/10.1007/s10533-022-00956-2, 2022.
602	Ji, Y., Zhao, Y., Han, X., Chen, X., Yan, J., Lu, X., Zhu, Y., Zou, W.: Effect of long-term
603	fertilization practices on the stability of soil organic matter in the northeast black soil
604	region in China, Agronomy, 14, 2272, https://doi.org/10.3390/agronomy14102272 , 2024.
605	Jindaluang, W., Kheoruenromne, I., Suddhiprakarn, A., Singh, B. P., Singh, B.: Influence of soil
606	texture and mineralogy on organic matter content and composition in physically
607	separated fractions soils of Thailand, Geoderma, 195–196, 207–219,
608	https://doi.org/10.1016/j.geoderma.2012.12.003, 2013.





609	Just, C., Armbruster, M., Barkusky, D., Baumecker, M., Diepolder, M., Döring, T. F., Heigl, L.,
610	Honermeier, B., Jate, M., Merbach, I., et al.: Soil organic carbon sequestration in
611	agricultural long-term field experiments as derived from particulate and
612	mineral-associated organic matter, Geoderma, 434, 116472,
613	https://doi.org/10.1016/j.geoderma.2023.116472, 2023.
614	Kleber, M., Eusterhues, K., Keiluweit, M., Mikutta, C., Mikutta, R., Nico, P. S.: Chapter one -
615	Mineral-organic associations: formation, properties, and relevance in soil environments,
616	in: Advances in Agronomy, Vol. 130, 1–140,
617	https://doi.org/10.1016/bs.agron.2014.10.005, 2015.
618	Kubar, K. A., Huang, L., Lu, J., Li, X., Xue, B., Yin, Z.: Long-term tillage and straw returning
619	effects on organic C fractions and chemical composition of SOC in rice-rape cropping
620	system, Arch. Agron. Soil Sci., 65, 125–137,
621	https://doi.org/10.1080/03650340.2018.1490726, 2018.
622	Lan, X., Shan, J., Huang, Y., Liu, X., Lv, Z., Ji, J., Hou, H., Xia, W., Liu, Y.: Effects of long-term
623	manure substitution regimes on soil organic carbon composition in a red paddy soil of
624	southern China, Soil Tillage Res., 221, 105395,
625	https://doi.org/10.1016/j.still.2022.105395, 2022.
626	Lavallee, J. M., Soong, J. L., Cotrufo, M. F.: Conceptualizing soil organic matter into particulate
627	and mineral-associated forms to address global change in the 21st century, Glob. Change
628	Biol., 26, 261–273, https://doi.org/10.1111/gcb.14859, 2020.





629	Li, Y., Li, Z., Cui, S., Liang, G., Zhang, Q.: Microbial-derived carbon components are critical for
630	enhancing soil organic carbon in no-tillage croplands: A global perspective, Soil Tillage
631	Res., 205, 104758, https://doi.org/10.1016/j.still.2020.104758, 2021.
632	Liang, G., Stark, J., Waring, B. G.: Mineral reactivity determines root effects on soil organic
633	carbon, Nat. Commun., 14, 4962, https://doi.org/10.1038/s41467-023-40768-y , 2023.
634	Ling, J., Dungait, J. A. J., Delgado-Baquerizo, M., Cui, Z., Zhou, R., Zhang, W., Gao, Q., Chen,
635	Y., Yue, S., Kuzyakov, Y., et al.: Soil organic carbon thresholds control fertilizer effects
636	on carbon accrual in croplands worldwide, Nat. Commun., 16, 3009,
637	https://doi.org/10.1038/s41467-025-57981-6, 2025.
638	Liu, L., Yang, J., Wang, J., Yu, Q., Wei, C., Jiang, L., Huang, J., Zhang, Y., Jiang, Y., Zhang, H., et
639	al.: Increase in mineral-associated organic carbon does not offset the decrease in
640	particulate organic carbon under long-term nitrogen enrichment in a steppe ecosystem,
641	Soil Biol. Biochem., 202, 109695, https://doi.org/10.1016/j.soilbio.2024.109695 , 2025.
642	Liu, Y., Ge, T., van Groenigen, K. J., Yang, Y., Wang, P., Cheng, K., Zhu, Z., Wang, J., Li, Y.,
643	Guggenberger, G., et al.: Rice paddy soils are a quantitatively important carbon store
644	according to a global synthesis, Commun. Earth Environ., 2, 154,
645	https://doi.org/10.1038/s43247-021-00229-0, 2021.
646	Liu, Y., Zhou, Z., Zhang, X., Xu, X., Chen, H., Xiong, Z.: Net global warming potential and
647	greenhouse gas intensity from the double rice system with integrated soil-crop system
648	management: A three-year field study, Atmos. Environ., 116, 92-101,
649	https://doi.org/10.1016/j.atmosenv.2015.06.018, 2015.





650	Lu, F., Wang, X., Han, B., Ouyang, Z., Duan, X., Hua, Z., Miao, H.: Soil carbon sequestrations by
651	nitrogen fertilizer application, straw return and no-tillage in China's cropland, Glob.
652	Change Biol., 15, 281–305, https://doi.org/10.1111/j.1365-2486.2008.01743.x , 2009.
653	Lu, R. K.: Analysis methods of soil agricultural chemistry, China Agricultural Science and
654	Technology Press, Beijing, (in Chinese), 2000.
655	Mao, H. R., Cotrufo, M. F., Hart, S. C., Sullivan, B. W., Zhu, X., Zhang, J., Liang, C., Zhu, M.:
656	Dual role of silt and clay in the formation and accrual of stabilized soil organic carbon,
657	Soil Biol. Biochem., 192, 109390, https://doi.org/10.1016/j.soilbio.2024.109390, 2024.
658	Mustafa, A., Frouz, J., Naveed, M., Ping, Z., Nan, S., Minggang, X., Núñez-Delgado, A.: Stability
659	of soil organic carbon under long-term fertilization: Results from ¹³ C NMR analysis and
660	laboratory incubation, J. Integr. Agric., 205, 112476,
661	https://doi.org/10.1016/j.envres.2021.112476, 2022.
662	Niu, Y., Li, Y., Lou, M., Cheng, Z., Ma, R., Guo, H., Zhou, J., Jia, H., Fan, L., Wang, T.: Microbial
663	transformation mechanisms of particulate organic carbon to mineral-associated organic
664	carbon at the chemical molecular level: Highlighting the effects of ambient temperature
665	and soil moisture, Soil Biol. Biochem., 195, 109454,
666	https://doi.org/10.1016/j.soilbio.2024.109454, 2024.
667	Oldfield, E. E., Bradford, M. A., Wood, S. A.: Global meta-analysis of the relationship between
668	soil organic matter and crop yields, Soil, 5, 15–32, https://doi.org/10.5194/soil-5-15-2019,
669	2019.
670	Panettieri, M., Knicker, H., Murillo, J. M., Madejón, E., Hatcher, P. G.: Soil organic matter
671	degradation in an agricultural chronosequence under different tillage regimes evaluated





672	by organic matter pools, enzymatic activities and CPMAS ¹³ C NMR, Soil Biol. Biochem.,
673	78, 170–181, https://doi.org/10.1016/j.soilbio.2014.07.021 , 2014.
674	Peng, Y., Biswas, A., Adamowski, J. F., Zhang, X., Li, Y., Li, L., Peng, Y., Cao, J.: Sources and
675	stability of particulate organic matter (POM) and mineral-associated organic matter
676	(MAOM) on the Loess Plateau: Implications for soil carbon management, Ecol. Indic.,
677	179, 114162, https://doi.org/10.1016/j.ecolind.2025.114162, 2025.
678	Rocci, K. S., Lavallee, J. M., Stewart, C. E., Cotrufo, M. F.: Soil organic carbon response to
679	global environmental change depends on its distribution between mineral-associated and
680	particulate organic matter: A meta-analysis, Sci. Total Environ., 793, 148569,
681	https://doi.org/10.1016/j.scitotenv.2021.148569, 2021.
682	Schmidt, M. W. I., Torn, M. S., Abiven, S., Dittmar, T., Guggenberger, G., Janssens, I. A., Kleber,
683	M., Kögel-Knabner, I., Lehmann, J., Manning, D. A. C., et al.: Persistence of soil organic
684	matter as an ecosystem property, Nat., 478, 49–56, https://doi.org/10.1038/nature10386 ,
685	2011.
686	Si, Q., Chen, K., Wei, B., Zhang, Y., Sun, X., Liang, J.: Dissolved carbon flow to particulate
687	organic carbon enhances soil carbon sequestration, Soil, 10, 441-450,
688	https://doi.org/10.5194/soil-10-441-2024, 2024.
689	Simon, C., Miltner, A., Mulder, I., Kaiser, K., Lorenz, M., Thiele-Bruhn, S., Lechtenfeld, O.:
690	Long-term effects of manure addition on soil organic matter molecular composition:
691	Carbon transformation as a major driver of energetic potential, Soil Biol. Biochem., 205,
692	109755, https://doi.org/10.1016/j.soilbio.2025.109755, 2025.





693	Six, J., Callewaert, P., Lenders, S., De Gryze, S., Morris, S. J., Gregorich, E. G., Paul, E. A.,
694	Paustian, K.: Measuring and understanding carbon storage in afforested soils by physical
695	fractionation, Soil Sci. Soc. Am. J., 66, 1981–1987,
696	https://doi.org/10.2136/sssaj2002.1981, 2002.
697	Stewart, C. E., Paustian, K., Conant, R. T., Plante, A. F., Six, J.: Soil carbon saturation: concept,
698	evidence and evaluation, Biogeochemistry, 86, 19–31,
699	https://doi.org/10.1007/s10533-007-9140-0, 2007.
700	Tan, B., Xiao, X., Yang, L., Meng, L., Li, S., An, N., Lu, Y., Wang, W., Han, W., Yi, Y.:
701	Mechanisms of soil structure stability in greenhouse: the balancing role of binding and
702	dispersing agents, J. Soils Sediments, 25, 2371–2386,
703	https://doi.org/10.1007/s11368-025-04079-7, 2025.
704	Vance, E. D., Brookes, P. C., Jenkinson, D. S.: An extraction method for measuring soil microbial
705	biomass C, Soil Biol. Biochem., 19, 703–707,
706	https://doi.org/10.1016/0038-0717(87)90052-6, 1987.
707	Vieira, F. C. B., Bayer, C., Zanatta, J. A., Dieckow, J., Mielniczuk, J., He, Z. L.: Carbon
708	management index based on physical fractionation of soil organic matter in an Acrisol
709	under long-term no-till cropping systems, Soil Till. Res., 96, 195–204,
710	https://doi.org/10.1016/j.still.2007.06.007, 2007.
711	Wiesmeier, M., Urbanski, L., Hobley, E., Lang, B., von Lützow, M., Marin-Spiotta, E., van
712	Wesemael, B., Rabot, E., Ließ, M., Garcia-Franco, N., et al.: Soil organic carbon storage
713	as a key function of soils - a review of drivers and indicators at various scales,
714	Geoderma, 333, 149–162, https://doi.org/10.1016/j.geoderma.2018.07.026 , 2019.





715	Witzgall, K., Vidal, A., Schubert, D. I., Höschen, C., Schweizer, S. A., Buegger, F., Pouteau, V.,
716	Chenu, C., Mueller, C. W.: Particulate organic matter as a functional soil component for
717	persistent soil organic carbon, Nat. Commun., 12, 4115,
718	https://doi.org/10.1038/s41467-021-24192-8, 2021.
719	Wu, B., Zhang, M., Zhai, Z., Dai, H., Yang, M., Zhang, Y., Liang, T.: Soil organic carbon, carbon
720	fractions, and microbial community under various organic amendments, Sci. Rep., 14,
721	25431, https://doi.org/10.1038/s41598-024-75771-w, 2024.
722	Xu, L., Wang, M., Tian, Y., Shi, X., Shi, Y., Yu, Q., Xu, S., Pan, J., Li, X., Xie, X.: Relationship
723	between macropores and soil organic carbon fractions under long-term organic manure
724	application, Land Degrad. Dev., 31, 1344–1354, https://doi.org/10.1002/ldr.3525, 2020.
725	Yan, H., Fan, W., Wu, J.: Effects of continuous manure application on the microbial community
726	and labile organic carbon fractions, Agriculture, 13, 2096,
726 727	and labile organic carbon fractions, Agriculture, 13, 2096, https://doi.org/10.3390/agriculture13112096 , 2023.
727	https://doi.org/10.3390/agriculture13112096, 2023.
727 728	https://doi.org/10.3390/agriculture13112096, 2023. Yang, L., Han, W., Tan, B., Wu, Y., Li, S., Yi, Y.: Effects of nutrient accumulation and microbial
727 728 729	https://doi.org/10.3390/agriculture13112096, 2023. Yang, L., Han, W., Tan, B., Wu, Y., Li, S., Yi, Y.: Effects of nutrient accumulation and microbial community changes on tomato fusarium wilt disease in greenhouse soil, Sustainability,
727 728 729 730	https://doi.org/10.3390/agriculture13112096, 2023. Yang, L., Han, W., Tan, B., Wu, Y., Li, S., Yi, Y.: Effects of nutrient accumulation and microbial community changes on tomato fusarium wilt disease in greenhouse soil, Sustainability, 16, 7756, https://doi.org/10.3390/su16177756, 2024.
727 728 729 730 731	https://doi.org/10.3390/agriculture13112096, 2023. Yang, L., Han, W., Tan, B., Wu, Y., Li, S., Yi, Y.: Effects of nutrient accumulation and microbial community changes on tomato fusarium wilt disease in greenhouse soil, Sustainability, 16, 7756, https://doi.org/10.3390/su16177756, 2024. Yao, B., Zeng, X., Pang, L., Kong, X., Tian, K., Ji, Y., Sun, S., Tian, X.: The photodegradation of
727 728 729 730 731 732	https://doi.org/10.3390/agriculture13112096, 2023. Yang, L., Han, W., Tan, B., Wu, Y., Li, S., Yi, Y.: Effects of nutrient accumulation and microbial community changes on tomato fusarium wilt disease in greenhouse soil, Sustainability, 16, 7756, https://doi.org/10.3390/su16177756, 2024. Yao, B., Zeng, X., Pang, L., Kong, X., Tian, K., Ji, Y., Sun, S., Tian, X.: The photodegradation of lignin methoxyl C promotes fungal decomposition of lignin aromatic C measured with
727 728 729 730 731 732 733	https://doi.org/10.3390/agriculture13112096, 2023. Yang, L., Han, W., Tan, B., Wu, Y., Li, S., Yi, Y.: Effects of nutrient accumulation and microbial community changes on tomato fusarium wilt disease in greenhouse soil, Sustainability, 16, 7756, https://doi.org/10.3390/su16177756, 2024. Yao, B., Zeng, X., Pang, L., Kong, X., Tian, K., Ji, Y., Sun, S., Tian, X.: The photodegradation of lignin methoxyl C promotes fungal decomposition of lignin aromatic C measured with 13C-CPMAS NMR, J. Fungi, 8, 900, https://doi.org/10.3390/jof8090900, 2022.

https://doi.org/10.5194/egusphere-2025-5094 Preprint. Discussion started: 3 November 2025 © Author(s) 2025. CC BY 4.0 License.





131	Zhang, Y., Hagedorn, F., Guidi, C., Yang, L.: Limited soil carbon storage under long-term organic
738	fertilization in solar greenhouses, Soil Use Manage., 38, 1614–1627
739	https://doi.org/10.1111/sum.12832, 2022.
740	Zhao, Z., Mao, Y., Gao, S., Lu, C., Pan, C., Li, X.: Organic carbon accumulation and aggregate
741	formation in soils under organic and inorganic fertilizer management practices in a
742	rice-wheat cropping system, Sci. Rep., 13, 3665
743	https://doi.org/10.1038/s41598-023-30541-y, 2023.
744	Zheng, W., Rao, C., Wu, Q., Wang, E., Jiang, X., Xu, Y., Hu, L., Chen, Y., Liang, X., Yan, W.
745	Changes in the soil labile organic carbon fractions following bedrock exposure rate in a
746	karst context, Forests, 13, 516, https://doi.org/10.3390/f13040516 , 2022.
747	Zhou, Z., Ren, C., Wang, C., Delgado-Baquerizo, M., Luo, Y., Luo, Z., Du, Z., Zhu, B., Yang, Y.
748	Jiao, S., et al.: Global turnover of soil mineral-associated and particulate organic carbon
749	Nat. Commun., 15, 5329, https://doi.org/10.1038/s41467-024-49743-7, 2024.
750	





751 **Table 1.** Manure application years and soil mechanical composition at greenhouse sampling sites.

Sampling	Manure application years	Points	Soil bulk density g cm ⁻³	pH 1:2.5	Sand %	Silt %	Clay %	Soil texture
	CK	3	1.12±0.03	7.06±0.23	43.6±1.5	21.0±1.8	35.4±1.7	
	2	3	1.19±0.06	6.98±0.22	43.7±3.0	20.7±3.3	34.9±0.9	
	9-11	4	1.13±0.03	7.05±0.19	42.3±1.6	20.9±2.8	36.8±4.1	
Wujianfang	20-23	3	1.15±0.04	7.00±0.15	42.6±1.5	23.3±1.9	34.1±2.0	Loam
Town	28-31	4	1.10±0.04	6.93±0.20	43.5±1.2	20.0±2.3	36.5±1.2	
	38-40	3	1.07±0.03	6.36±0.21	43.2±1.7	20.7±2.5	36.1±2.2	
	48-50	3	1.14±0.06	6.60±0.13	44.4±1.0	19.6±0.9	36.0±1.3	
	CK	3	1.24±0.03	6.42±0.24	70.9±2.1	8.2±1.9	20.9±2.8	
	2	3	1.25±0.03	6.84±0.23	70.1±3.0	8.6±0.9	21.3±3.1	
Yangshipu	4-6	3	1.27±0.01	7.02±0.33	70.6±2.6	8.3±2.7	21.1±0.9	Sandy
Town	11-13	3	1.23±0.02	7.15±0.28	70.43±2.6	9.4±0.9	20.2±2.1	Loam
	21-24	3	1.21±0.01	7.09±0.06	69.4±2.7	7.1±1.5	23.5±4.2	
	30-32	4	1.25±0.04	7.14±0.24	68.7±2.6	7.5±1.4	23.9±3.5	





Table 2. Percentage (%) contributions of C functional groups based on integrated CPMAS 13C NMR spectroscopy of bulk soil in the greenhouse.

Table 2. F	ercentage (70) et	Julibulions of C	Table 2. reicentage (70) continuations of C functional groups based on integrated Crimas TC inmix specifiescipy of durk son in the greathouse.	sa on megi	alcu of MAS		specuoscopy or	ouik soii iii u	in greenin	onse.		
Soil texture Treatment	Treatment	Alkyl C	O-Alk	O-Alkyl C (45-110 ppm)	(0 ppm)		Aromatic C	Aromatic C (110-160 ppm)	m)	Carbony	Carbonyl C (160-220 ppm)	(mdd
	years	(0-45 ppm)	N-alkyl/methoxyl	O-alkyl	di-O-alkyl	Ę	Aryl C/O-aryl	- -	E		, ,	-
			Ü	C	C	I Otal	C	Phenolic-C	Iotal	Amide-C	Amide-C Ketone-C	lotal
	CK	42.40	8.70	20.82	2.31	31.83	7.88	5.90	13.78	6.75	5.24	11.99
1	2 yr	34.20	7.78	19.73	4.29	31.80	10.56	7.75	18.31	8.89	6.79	15.68
LOAIII	9–11 yr	28.55	4.71	14.31	4.22	23.24	16.62	9.54	26.16	12.81	9.25	22.05
	28–31 yr	31.16	3.81	7.74	3.60	15.15	19.89	11.34	31.23	12.82	9.65	22.46
	CK	25.67	6.67	22.34	6.63	35.65	13.92	5.65	19.57	13.00	6.11	19.11
Sandy	2 yr	30.58	8.16	17.72	6.73	32.62	13.91	4.51	18.42	14.23	4.16	18.39
Loam	11–13 yr	38.54	8.90	13.05	7.46	29.42	12.01	2.30	14.31	13.66	4.07	17.73
	30–32 yr	37.54	8.88	13.14	7.50	29.52	12.13	2.45	14.58	12.88	4.86	17.74

756

757

758



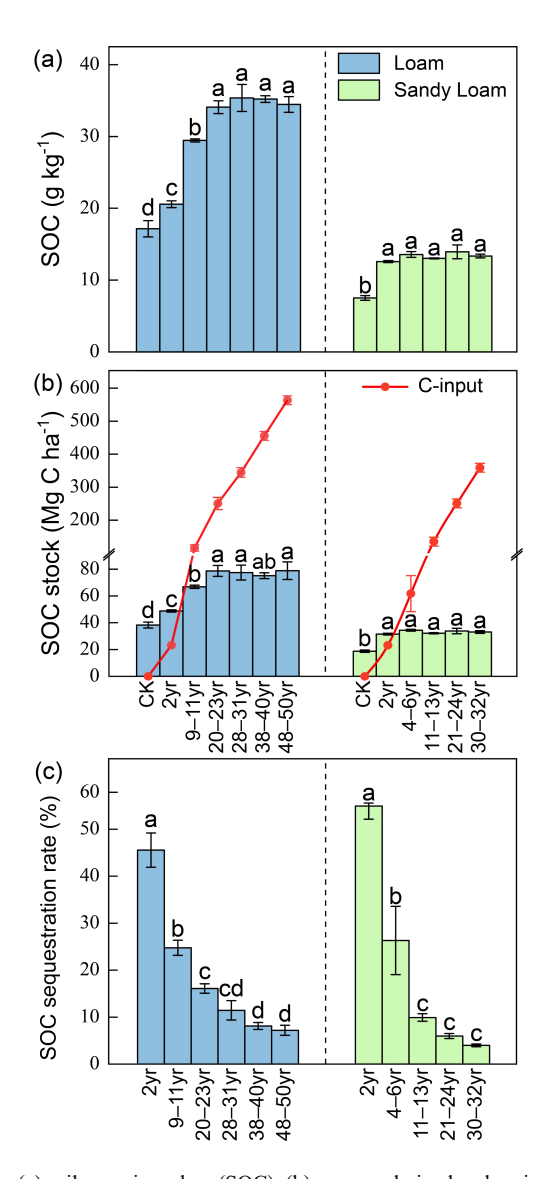


Fig. 1. Changes in (a) soil organic carbon (SOC), (b) manure-derived carbon input and SOC stock, and (c) SOC sequestration rate following manure application over various years in greenhouses. Bars represent the standard errors. Within each soil texture, bars with different lowercase letters indicate significant differences among years of manure application (P < 0.05).



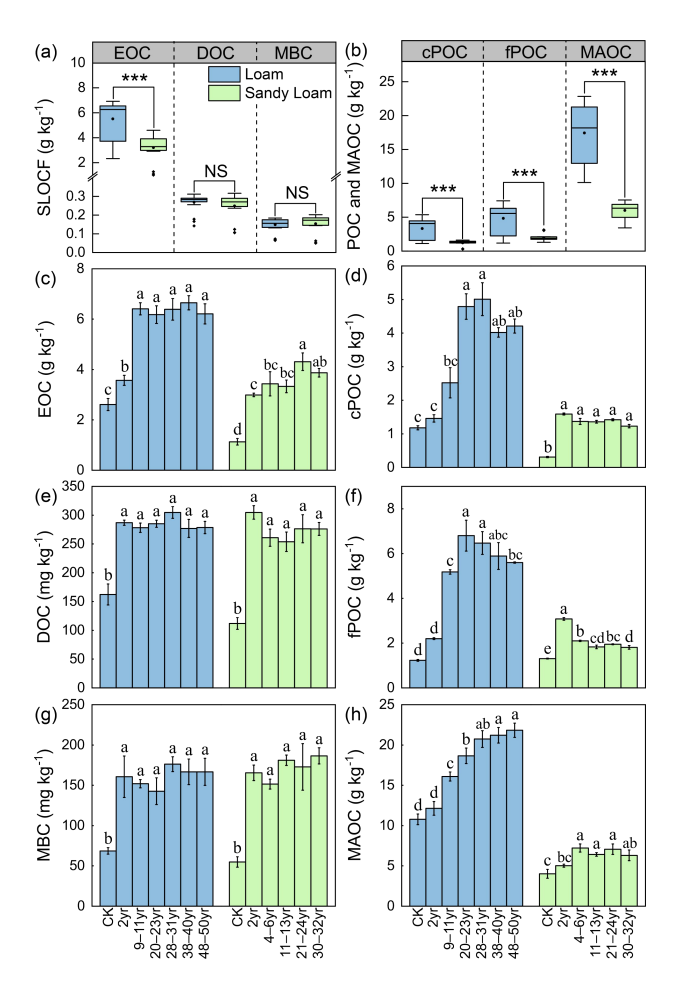


Fig. 2. Content and variations of (a) soil labile organic carbon fractions (SLOCF), (b) particulate organic carbon (POC), and mineral-associated organic carbon (MAOC) in greenhouse soils (loam and sandy loam); and dynamic changes in (c) easily oxidizable organic carbon (EOC), (e) dissolved organic carbon (DOC), (g) microbial biomass carbon (MBC), (d) coarse particulate organic carbon (cPOC), (f) fine particulate organic carbon (fPOC), and (h) mineral-associated organic carbon (MAOC) across different years of manure application in greenhouse soils. Bars represent the standard errors. Within each soil texture, bars with different lowercase letters indicate significant differences among years of manure application (P < 0.05).





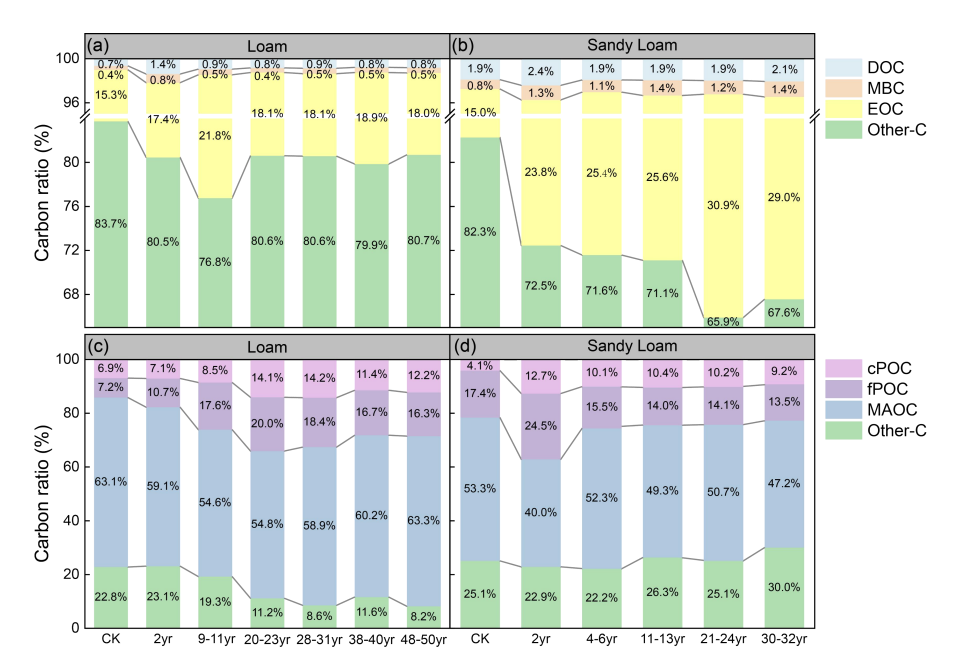


Fig. 3. Proportions of soil labile organic carbon fractions (SLOCF: easily oxidizable organic carbon [EOC], microbial biomass carbon [MBC], and dissolved organic carbon [DOC]), particulate organic carbon (POC: coarse POC [cPOC] and fine POC [fPOC]), and mineral-associated organic carbon (MAOC) to soil organic carbon (SOC) in greenhouse soils under different manure application years in (a, c) loam and (b, d) sandy loam.





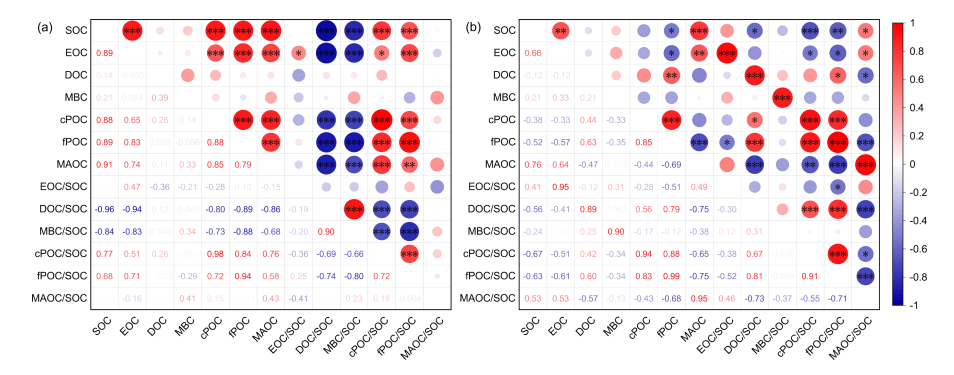


Fig. 4. Pearson correlations among soil organic carbon (SOC) fractions and their relative proportions in greenhouses for (a) loam and (b) sandy loam. Note: SOC fractions include total SOC, easily oxidizable organic carbon (EOC), dissolved organic carbon (DOC), microbial biomass carbon (MBC), coarse particulate organic carbon (cPOC), fine particulate organic carbon (fPOC), and mineral-associated organic carbon (MAOC). Their relative proportions to SOC include EOC/SOC, DOC/SOC, MBC/SOC, cPOC/SOC, fPOC/SOC, and MAOC/SOC. *

Correlation was significant at $P \leq 0.05$; ** Correlation was significant at $P \leq 0.01$; ***





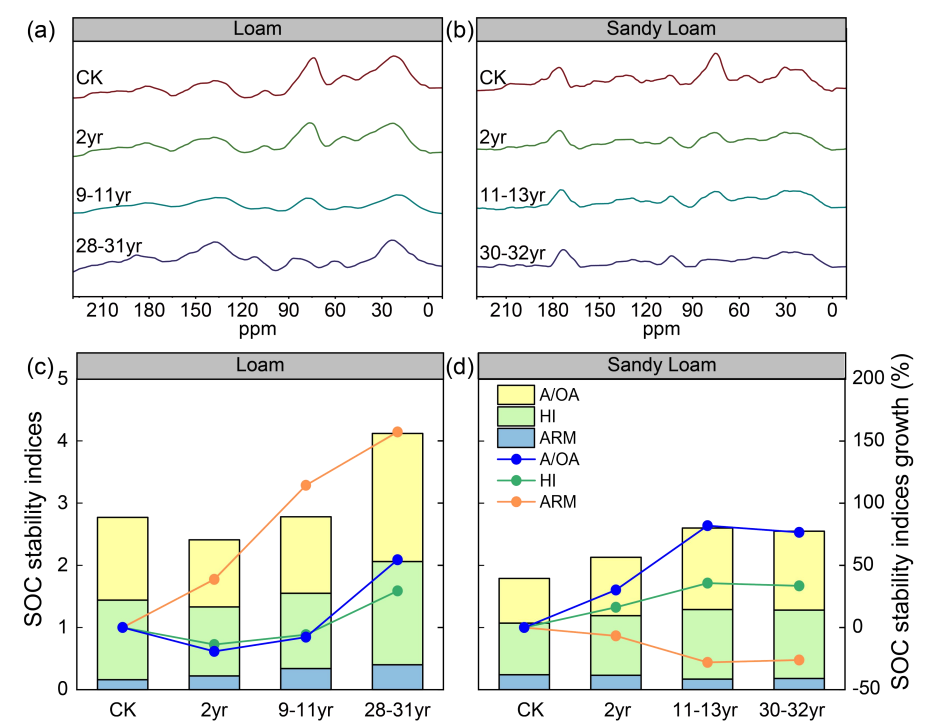


Fig. 5. Solid-state CPMAS ¹³C NMR spectroscopy of greenhouse soils under varying years of manure application in (a) loam and (b) sandy loam. Soil organic carbon (SOC) stability indicators during different manure application years in (c) loam and (d) sandy loam under greenhouse conditions. A/OA: the ratio of alkyl C to O-alkyl; HI: hydrophobicity index; ARM: aromaticity index.





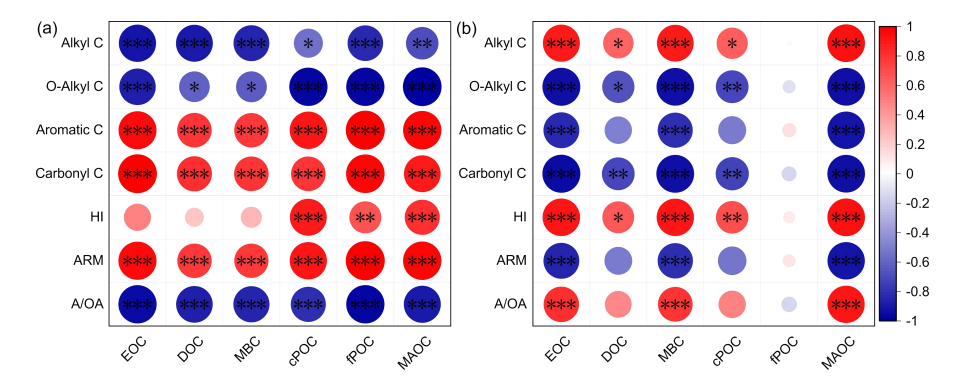


Fig. 6. Pearson correlations between soil organic carbon (SOC) fractions and SOC chemical structure and stability indices in greenhouses (a) loam and (b) sandy loam. Note: SOC fractions include total SOC, easily oxidizable organic carbon (EOC), dissolved organic carbon (DOC), microbial biomass carbon (MBC), coarse particulate organic carbon (cPOC), fine particulate organic carbon (fPOC), and mineral-associated organic carbon (MAOC). SOC stability indices include aromaticity index (ARM), humification index (HI), and the ratio of alkyl C to O-alkyl (A/OA). * Correlation was significant at $P \le 0.001$; ***
Correlation was significant at $P \le 0.001$.



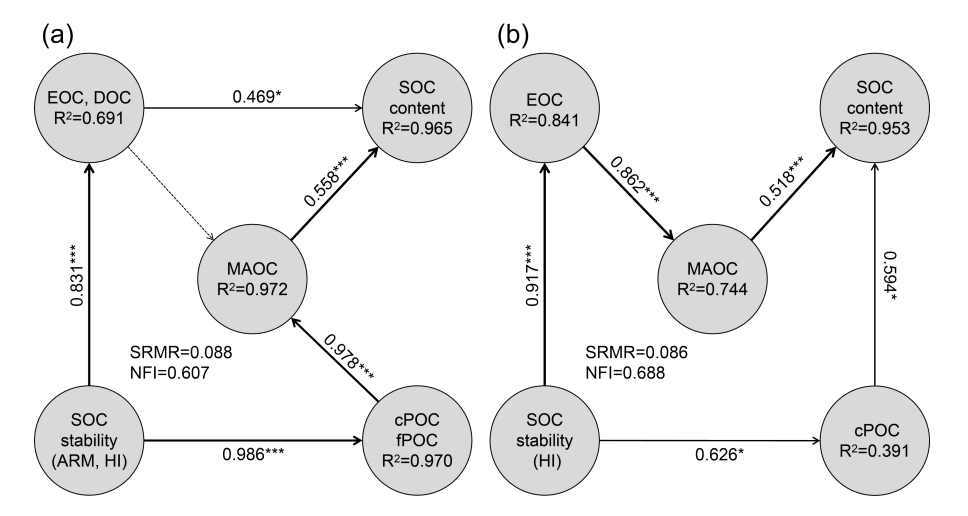


Fig. 7. Partial least squares structural equation models (PLS-SEM) illustrating the pathways through which soil organic carbon (SOC) chemical stability indices influence SOC fractions and SOC content in greenhouse soils: (a) loam; (b) sandy loam. Numbers on arrows denote path coefficients, while numbers adjacent to arrows represent weight contributions. Solid and dashed lines indicate significant and non-significant relationships, respectively. Note: SOC fractions include easily oxidizable organic carbon (EOC), dissolved organic carbon (DOC), coarse particulate organic carbon (ePOC), fine particulate organic carbon (fPOC), and mineral-associated organic carbon (MAOC). SOC chemical stability indices include aromaticity index (ARM) and humification index (HI).